Received 23 November 2020 ; revised 15 February 2021; accepted 12 March 2021. Date of publication 17 March 2021; date of current version 26 March 2021.
The review of this article was arranged by Editor C. Surya.

Digital Object Identifier 10.1109/JEDS.2021.3066369

High *Q* Lateral-Field-Excited Bulk Resonator Based on Single-Crystal $LiTaO_3$ for 5G Wireless Communication

YANMEI XUE [1], XIAODONG YANG [1], CHANGJIAN ZHOU [1] (Senior Member, IEEE), XIU YIN ZHANG [1] (Senior Member, IEEE), AND MANSUN CHAN [2] (Fellow, IEEE)

1 School of Electronic and Information Engineering, South China University of Technology, Guangzhou 510641, China
2 Department of Electronic and Computer Engineering, Hong Kong University of Science and Technology, Clear Water Bay, Hong Kong

CORRESPONDING AUTHORS: C. ZHOU AND X. ZHANG (e-mail: zhoucj@scut.edu.cn; zhangxiuyin@hotmail.com)

This work was supported in part by the National Natural Science Foundation of China under Grant 11804102; in part by the International Science & Technology Cooperation Program of Guangdong Province under Grant 2019A050510011; in part by the Science and Technology Program of Guangzhou under Grant 201807010072; in part by the Guangdong Pearl River Youth Talent Recruitment Program; and in part by Guangdong Basic and Applied Basic Research Foundation under Grant GDSTI19EG20.

ABSTRACT The paper presents the design and fabrication of lateral-field-excited (LFE) resonators based on 42° Y-cut single-crystal $LiTaO_3$ (LT) on silicon dioxide (SiO_2). A simple coplanar top electrode is defined to excite the bulk acoustic wave modes in the suspended LT/SiO_2 structure, and the fabrication process that only involves two lithography steps is more simplified compared to that of commercial film bulk acoustic wave resonators. For a model structure consisting of LT(670 nm)/SiO_2 (1500 nm) thin film, two types of acoustic modes are both piezoelectrically active in the LT film: the first one is the thickness-shear mode with a resonance frequency of 2.46 GHz, an electromechanical coupling (k^2_{eff}) of 1.4%, a high quality factor (Q) of 1690, and the second one corresponds to longitudinal mode with a resonance frequency of 4.39 GHz, k^2_{eff} of 1.2%, a high Q of 1590, which is among the highest reported for piezoelectric MEMS resonators operating at this frequency range. The excellent performance would enable application scenarios including high-resolution sensors, low-phase-noise oscillators, and low-loss, high selectivity filters in the sub-6 GHz range for the fifth-generation (5G) wireless communication.

INDEX TERMS Lateral field excitation, single-crystal $LiTaO_3$, shear mode, longitudinal mode, 5G wireless communication.

I. INTRODUCTION

With the development of large-volume and high-speed communication systems in the past decades, there is an ever-increasing demand for high-frequency acoustic devices. For example, the emerging 5G wireless communication system targets operation in the super-high-frequency (SHF) band (3-30 GHz). Currently, for frequency above 3 GHz, the mainstream filters used in wireless communication systems are film bulk acoustic wave resonators (FBARs) [1], where the thickness-extention mode (TEM) is utilized to obtain a relatively wide bandwidth. However, enhancement of the operating frequency is an actual challenge for the electrode/piezoelectric/electrode FBAR structure, since the added electrode thickness reduces the resonance frequency and this is extremely important especially for future high-frequency resonator which requires a piezoelectric thin film with a thickness comparable to that of the electrode.

In recent years, shear mode bulk acoustic wave that can be readily excited with the lateral-field-excited (LFE) resonators has attracted great attention related to liquid-phase sensing applications [2]–[4]. The absence of the surface-normal displacement allows the shear mode wave to propagate in the liquid environment without coupling energy into the liquid compared to the TEM wave. In LFE resonators, the acoustic waves are excited between the coplanar electrodes, but the electrodes themselves are not in the acoustic wave transport path which helps to reduce acoustic attenuation and increase the resonance frequency [5], [6]. What is more, the

coplanar electrodes are patterned on top of the piezoelectric thin film, which promises a simpler fabrication process and a lower cost.

Besides, current commercial acoustic wave devices widely utilize aluminum nitride (AlN) and zinc oxide (ZnO) deposited using sputtering techniques as piezoelectric materials owing to their low cost and high growth rates. However, when the thickness of the polycrystalline thin film is reduced to sub-micron, due to the damping mechanisms intrinsic to the polycrystalline thin films including the grain boundary scattering losses, the crystal quality becomes worse and the intrinsic acoustic attenuation effect manifest itself, leading to a low Q as well as reduced coupling coefficient (k^2_{eff}) of the fabricated resonators. For example, previous works on LFE resonators used ZnO or AlN as the piezoelectric thin films [7]–[11]. The Q values of the LFE resonators in [7], [8] are less than 400, and the k^2_{eff} in [9], [10] is within 0.5%, which are still much inferior to that of the FBARs and aren't acceptable for low-loss filter applications.

Compared with FBARs with piezoelectric thin films sandwiched by electrodes, LFE resonator does not require a bottom electrode, thus enabling the use of single-crystal piezoelectric thin films. Since the quality of the piezoelectric thin films is of great importance to fabricate a high-performance resonator, single-crystal films with a highly organized microstructure, good piezoelectric properties could substantially improve the resonator performances. Up to now, there have been few studies on single-crystal piezoelectric thin films for high-frequency bulk acoustic resonators.

In this paper, 42° Y-cut crystal LT is selected as the model piezoelectric thin film for LFE resonators. Among commercial available single-crystal piezoelectric materials, LT offers high wave velocity and large k^2_{eff} but poor temperature stability in the range of around −30 to −45 ppm/°C [12]. Hence additional SiO_2 underlayer is integrated for temperature stabilization. When the opposing electrodes in LFE resonator are connected to signal and ground, respectively, the lateral alternating electric field is induced in the mechanically suspended LT thin film.

Two main propagation modes at 2.46 GHz and 4.39 GHz are excited with Q of 1690 and 1590, respectively. They are defined as the thickness-shear mode for the first mode and thickness-extention mode for the second mode, according to the theoretical calculation of velocities and vibration mode shapes simulated with finite element analysis. The LFE resonators with a high frequency and a high Q, enable them strong candidates for high-resolution sensors, low-phase-noise oscillators and low-loss narrowband filters for radio frequency wireless communication, such as LTE-Advanced contiguous carrier aggregation which requires up to 20 MHz bandwidth [13] and IEEE 802.11a wireless LAN system occupying 16.6 MHz at a center frequency of 5 GHz [14].

II. RESONATOR FABRICATION

In this study, the LFE resonators require only one layer of metallization for electrodes, evidently simplifying the fabrication process compared with traditional FBARs. Meanwhile, without a bottom electrode, a single-crystal piezoelectric thin film with superior electrical properties can be prepared atop the substrate for high-frequency resonator fabrications.

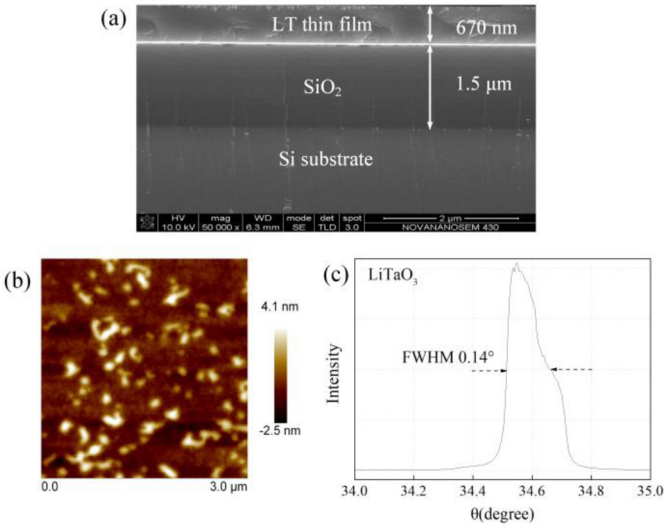

FIGURE 1. (a) Scanning electron microscopy cross-sectional image of LT/SiO_2/Si layered structure; (b) Atomic force microscopy image of the LT thin film with a scanning area of 3μm×3μm; (c) XRD rocking curve of the LT film.

A commercial wafer from NANOLN with 42°Y-cut single-crystal piezoelectric LT (0.67 μm-thick) film and silicon oxide (1.5 μm-thick) film on top of a Si substrate (300 μm-thick) is adopted. Fig. 1(a) presents the cross-sectional scanning electron microscope (SEM) image of the substrate before releasing, in which each layer can be clearly observed, revealing the single-crystalline piezoelectric thin films with clean interfaces and low scattering loss. The root mean square roughness of the LT film is about 1.06 nm over the measured range of 3 μm×3 μm, as shown in Fig. 1(b), ensuring a smooth surface for the fabrication of LFE devices. X-ray diffraction (XRD) rocking curve of the single-crystal LT film, which corresponds to 42° Y-cut orientation of the crystal structure, is shown in Fig. 1(c). The full width at half maximum (FWHM) value is approximately 0.14°, indicating the near-perfect LT crystal formation.

Fig. 2 (a) shows the fabrication process flow, which consists of two photolithography steps and two etching/releasing steps. To release the resonator structure, an etching window pattern is firstly defined by the first lithography step. Then the silicon substrate in the etching window is exposed by anisotropic dry etching of the LT/SiO_2 upper layers. LT is a notoriously inert piezoelectric material just like $LiNbO_3$, which makes it a great challenge to etch LT with smooth surfaces and straight sidewalls while preserving a high etching rate.

In this work, this was achieved through the optimization of a Cl_2/BCl_3 based ICP recipe. To be more specific, for

the ICP etching, the Cl_2/BCl_3 flow rate was 5/25 sccm, the ICP power is 600 W, the AZ4620 photoresist is used as the etching mask, and the chamber temperature is modified from 70 °C to −20 °C for the photoresist-based etching recipe. In addition, the etching process is intermittently paused for five minutes after 10 minutes of etching. It takes approximately 22 minutes without counting the pause time to define the etching windows and the photoresist didn't get burned in the low-temperature process.

Next, the coplanar Cr 10nm/Pt 100nm electrodes are formed on the LT thin film by the second photolithography step, which is followed by the metal deposition and lift-off process to define the G-S-G electrodes. Finally, the silicon substrate underneath the resonator was removed through XeF_2 isotropic dry etching to create suspended structures from the host Si substrate. The final resonator structure is shown in Fig. 2(b). The dark black region denotes the etching window, and the grey area around releasing holes depicts the air cavity of the etched silicon substrate, indicating the sacrificial layer was isotropically etched. The platinum electrodes with a two-port G-S-G structure are deposited and patterned by the conventional photolithography method for the following on-chip characterizations. The length, width, and gap of the parallel electrodes are designed to be 100μm, 15μm, and 10μm respectively. The resonant structures are fully suspended without substantial bending or cracking, representing the absence of high residual stress in the released thin film.

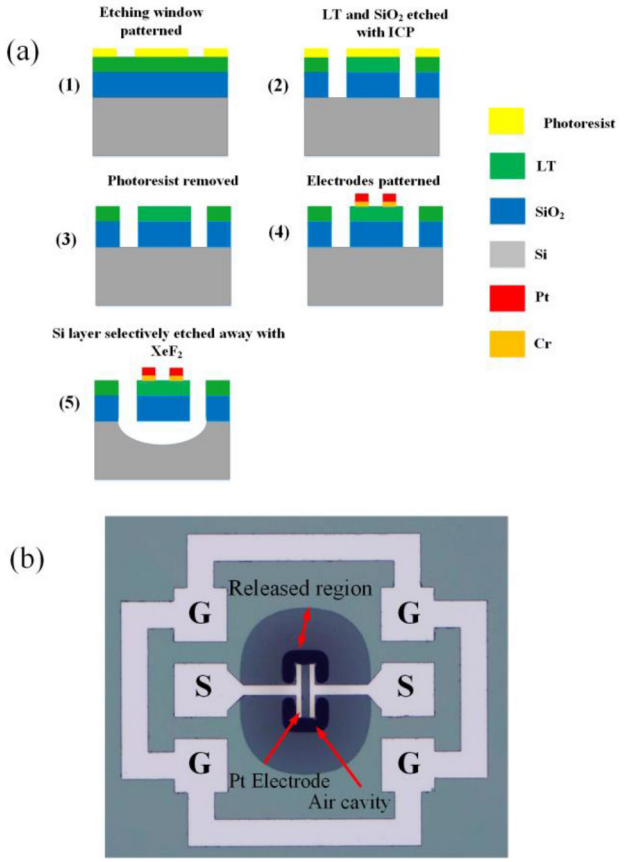

FIGURE 2. (a) Fabrication process flow of Y-cut $LiTaO_3$ LFE resonators; (b) Microscope image of the LFE resonator, where the length, width and gap of the electrodes are 100μm, 15μm and 10μm respectively.

III. RESULTS AND DISCUSSION

The microfabricated LFE resonators were characterized by the Agilent network analyzer (N5224A), and the on-chip measurement was conducted on a Cascade RF probe station. During the measurement, the scanned frequency is firstly set at a large range to obtain the acoustic mode frequency, then narrowed to achieve a 31 kHz frequency step size to obtain an accurate calculation of Q and k_{eff}^2.

A. RESONANT MODE ANALYSIS AND THE MEASUREMENT OF ELECTROMECHANICAL COUPLING (K_{EFF}^2) AND QUALITY FACTOR (Q)

The measured two-port scattering parameters S_{21} is shown in Fig. 3(a), presenting two major resonances (mode I, mode II) at 2.46 GHz and 4.39 GHz. We denote the main modes as shear and longitudinal bulk wave fundamental mode, and the velocity is simply calculated as $v_0 = f_0 \times 2d$, with d being the thickness of the LT film. The calculated two major resonances velocities are 3296 m/s and 5883 m/s, respectively. We compare these calculation parameters to the shear and longitudinal velocities of LT film in [15] to verify the type of mode. They agree quite well, but our calculated velocities from measurement are slightly smaller. Considering the imprecision in the thickness of LT film, the deviation is acceptable. Hence the two major resonances are verified to be thickness-shear mode and thickness-extention mode, respectively.

In addition, we performed a finite element simulation (FEM) analysis to gain further insight into the piezoelectric generation of acoustic waves and examined resulting particle displacements. As shown in Fig. 3(b), the first lateral mode is excited by the adjacent electrode and the distribution of the amplitude of displacement confirms that the acoustic energy is concentrated in the lateral center of the resonator body, while the second longitudinal mode is excited under the electrode. The vibration mode shapes further identify the type of acoustic modes. It's also noticed part of energy leaks into the SiO_2 layer, demonstrating the amorphous SiO_2 material can bring in extra acoustic attenuation.

The S-parameter of LFE resonators are measured again over a narrow frequency range to obtain the k_{eff}^2 and Q. The experimental coupling coefficients k_{eff}^2 are 1.4% and 1.2%. Meanwhile, the Q estimated by the slope of impedance phase [16] reaches a value of 1690 for the TSM and 1590 for the TEM, marking the high Q demonstrated for acoustic-only resonators in the sub-6 GHz band. In terms of quality factor and coupling efficiencies, there are discrepancies between the simulated results and the measured ones. These discrepancies can be attributed to deviations between material constants used in theoretical analysis and those of the fabricated

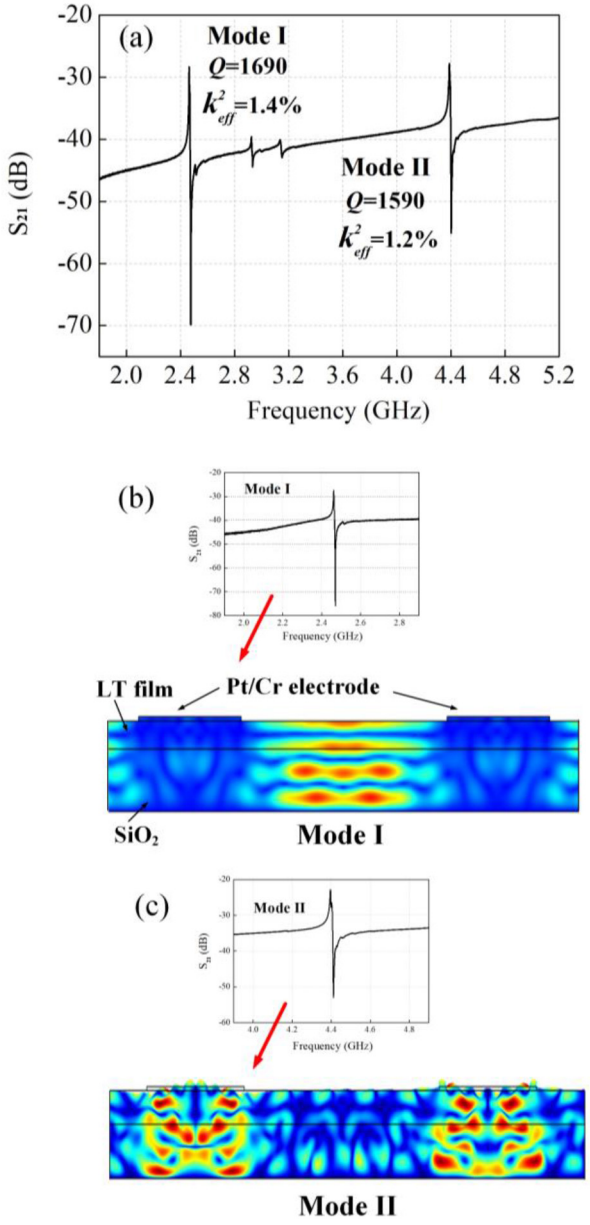

FIGURE 3. **(a) Measured S_{21} frequency response of the fabricated Y-cut $LiTaO_3$ LFE resonators; (b)-(c): The zoomed-in peaks in S-parameter and simulated displacement mode shapes of mode I, mode II.**

piezoelectric films, and the simplified 2D FEM model using infinite boundary conditions and one pair of electrodes. Thus, we focus more on the acoustic energy displacement during the FEM analysis.

The measured results of the proposed LFE resonators are compared against prior LFE resonators using sputtering piezoelectric films in Table 1, showing high working frequencies along with the remarkable high *Q*. Such high *Q* is due to the combined results of the use of the lossless single-crystal LT film as well as the LFE electrode. As the electrodes have practically no vibrations inside them and thus the usually-high acoustic loss in the metal electrode can be avoided. They are sufficient to support high-frequency and low-loss filtering operation towards the 5G marketplace.

TABLE 1. **Performance comparison with some prior LFE resonators.**

Ref.	Materials	Freq (GHz)	*Q*	k_{eff}^2(%)	$Q \times k_{eff}^2$	$f \times Q$ (GHz)
[7]	Sputtered ZnO	1.46	398	4.43	17.6	581.1
[8]	Sputtered AlN	1.948.	405	~1.2	4.9	788.9
[9]	Sputtered ZnO	2.59	1957	0.48	7.7	5068.6
[10]	Sputtered AlN	1.86	870	0.15	1.3	1618.2
[11]	Sputtered MgZnO	2.046	965	2.5	24	1974.4
This work	**Single crystalline $LiTaO_3$**	**2.46**	**1690**	**1.4**	**23.7**	**4157.4**
		4.39	**1590**	**1.2**	**19.1**	**6980.1**

In the measured spectrum, there are two parasitic modes located at roughly 2.9 and 3.1 GHz, as well as a relatively weaker spurious mode near the first main wave mode. The weak spurious wave mode is at least 15 dB lower than the main wave mode, thus we infer that it will not cause too much energy loss. The other two spurious modes are relatively far from the main modes. These features are advantageous for constructing high-resolution sensors and low-loss filters based on the LFE resonators. It should be noted in idealized models, the LFE configurations ignore fringing fields at the edges of the coplanar electrodes. In real devices, however, the electric field excited by top electrodes is non-uniform, the non-uniform electric field becomes the origins and results in unwanted spurious modes in addition to the desired pure modes. Therefore, we believe the measured *Q* and k_{eff}^2 can be further optimized if these unwanted modes can be suppressed.

B. THE DEPENDENCY OF RESONANCE FREQUENCY ON TEMPERATURE

For practical applications, the resonators should maintain their performances over a specified range of operating temperatures. To determine the temperature coefficient of the frequency (TCF) of the LFE resonator, the S parameters are obtained in the temperature range from 20°C to 90°C. The temperature was varied at 10°C/step and measurement at each temperature is conducted when the temperature is stabilized.

Fig. 4(a)–(b) show the S_{21} curves of the two main modes at different temperatures, showing the resonator's performance under each temperature condition, such as *Q* and k_{eff}^2, remain almost unaltered. The relationship between the resonance frequency and temperature is nearly linear, which shows a high uniformity of TCF in the measured temperature range as demonstrated in Fig. 4(c)–(d). It is derived from the test results that the TCF of the TSM and TEM waves is about −20 and −18 ppm/°C, respectively. Given the fact

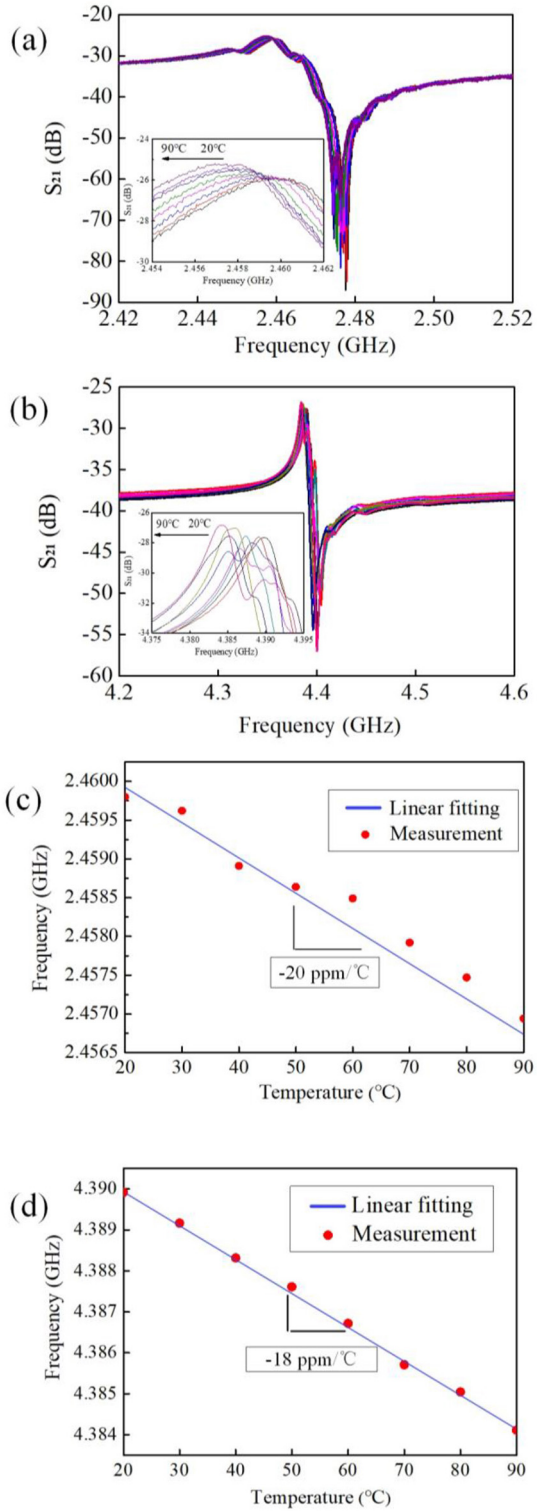

FIGURE 4. Measured S_{21} parameters of the fabricated LFE resonator from 20°C to 90°C for (a) mode I and (b) mode II ; The extracted relation of resonance frequency and temperature for (c) mode I and (d) mode II.

that the uncompensated LT materials display a rather large and negative TCF of approximately −40 ppm/°C, the results clearly show the advantage of the integrated silicon oxide for temperature compensation.

The relatively thick SiO_2 underlay not only provides temperature compensation but also considerably degrades Q because of the inevitable energy loss in the amorphous SiO_2 material [17]. Therefore, there exists a trade-off between the TCF, coupling coefficient and Q. However, considering near-zero TCF in certain cut angle for thickness mode [18], and as illustrated in [19], if the SiO_2 layer is deposited on the top electrodes, the reduction of TCF is obtained with thicker SiO_2 layer but the reduction in coupling coefficient is lower, hence we believe much freedom is left for further improving the TCF, enabling the single-crystal $LiTaO_3$ based LFE resonators better candidates for frequency-stable acoustic devices for 5G wireless communication.

IV. CONCLUSION

In conclusion, the lateral-field-excited resonators based on 42°Y-cut single-crystal $LiTaO_3$ thin film were designed and fabricated. Both thickness-shear mode at 2.46 GHz and thickness-extention mode at 4.39 GHz are excited, verified by experimental measurement and FEM simulation. The fabricated resonators demonstrate a Q of 1690 and 1590 for the two modes, respectively, exceeding current LFE acoustic resonators operating at the same sub-6 GHz frequency range. The measured values can be further optimized and future work will focus on enhancing Q and k_{eff}^2 by suppressing spurious modes and optimizing SiO_2 film to restrict energy loss. Moreover, with the fast development of the ultra-thin single-crystal piezoelectric thin films, the design and fabrication strategies can be further extended to the super-high-frequency band (3-30 GHz) for 5G mobile communication systems.

REFERENCES

[1] C. C. W. Ruppel, "Acoustic wave filter technology—A review," *IEEE Trans. Ultrason., Ferroelectr., Freq. Control*, vol. 64, no. 9, pp. 1390–1400, Sep. 2017.

[2] D. Chen, J. Wang, and Y. Xu, "Highly sensitive lateral field excited piezoelectric film acoustic enzyme biosensor," *IEEE Sensors J.*, vol. 13, no. 6, pp. 2217–2222, Jun. 2013.

[3] B. D. Zaitsev, I. E. Kuznetsova, A. M. Shikhabudinov, O. V. Ignatov, and O. I. Guliy, "Biological sensor based on a lateral electric field-excited resonator," *IEEE Trans. Ultrason., Ferroelectr., Freq. Control*, vol. 59, no. 5, pp. 963–969, May 2012.

[4] Y. Fu *et al.*, "Advances in piezoelectric thin films for acoustic biosensors, acoustofluidics and lab-on-chip applications," *Progr. Mater. Sci.*, vol. 89, pp. 31–91, Aug. 2017.

[5] A. Ballato, E. R. Hatch, M. Mizan, T. Lukaszek, and E. R. Tilton, "Simple thickness plate modes driven by lateral fields," in *Proc. 39th Annu. Freq. Control Symp.*, Philadelphia, PA, USA, 1985, pp. 462–472.

[6] Y. F. Zhang and D. Chen, *Multilayer Integrated Film Bulk Acoustic Resonators*. Berlin, Germany: SJTU Press, 2012.

[7] S. H. Meng, A. C. Huang, Y. C. Chen, and C. Yuan, "Lateral field excitation of thickness longitudinal mode and shear mode with ZnO based on solidly mounted resonator," *IEEE Trans. Ultrason., Ferroelect., Freq. Control*, vol. 66, no. 5, pp. 1014–1021, May 2019.

[8] D. Chen, W. Ren, S. Song, J. Wang, W. Liu, and P. Wang, "The high Q factor lateral field–excited thickness shear mode film bulk acoustic resonator working in liquid," *Micromachines*, vol. 7, no. 12, p. 231, Dec. 2016.

[9] A. D. Wathen, F. Munir, and W. D. Hunt, "A high-*Q* hybrid acoustic mode in thin film ZnO solidly mounted resonators," *Appl. Phys. Lett.*, vol. 95, Sep. 2009, Art. no. 123509.

[10] E. Milyutin, S. Gentil, and P. Muralt, "Shear mode bulk acoustic wave resonator based on *c*-axis oriented AlN thin film," *J. Appl. Phys.*, vol. 104, Aug. 2008, Art. no. 084508.
[11] Y. Liu *et al.,* "Solidly mounted resonators fabricated for GHz frequency applications based on $Mg_xZn_{1-x}O$ piezoelectric film," *Vacuum*, vol. 141, pp. 254–258, Jul. 2017.
[12] T. Bauer, C. Eggs, K. Wagner, and P. Hagn, "A bright outlook for acoustic filtering: A new generation of very low-profile SAW, TC SAW, and BAW devices for module integration," *IEEE Microw. Mag.*, vol. 16, no. 7, pp. 73–81, Aug. 2015.
[13] R. Ratasuk, D. Tolli, and A. Ghosh, "Carrier aggregation in LTE-advanced," in *Proc. IEEE 71st Veh. Technol. Conf.*, Taipei, Taiwan, 2010, pp. 1–5.
[14] H.-Y. Tsui and J. Lau, "A 5GHz 56dB voltage gain 0.18μm CMOS LNA with built-in tunable channel filter for direct conversion 802.11a wireless LAN receiver," in *Proc. IEEE Radio Freq. Integr. Circuits Symp. (RFIC)*, Philadelphia, PA, USA, 2003, pp. 225–228.
[15] M. Gonzalez, "Impact of Li non-stoichiometry on the performance of acoustic devices on LiTaO3 and LiNbO3 single crystals," Ph.D. dissertation, Dept. Chem. Phys., Univ. Franche-Comté, Besançon, France, 2017.
[16] W. Pang, H. Zhang, and E. S. Kim, "Micromachined acoustic wave resonator isolated from substrate," *IEEE Trans. Ultrason., Ferroelect., Freq. Control*, vol. 52, no. 8, pp. 1239–1246, Aug. 2005.
[17] H. Zhang, Q. Yang, W. Pang, J.-G. Ma, and H. Yu, "Temperature stable bulk acoustic wave filters enabling integration of a mobile television function in UMTS system," *IEEE Microw. Wireless Compon. Lett.*, vol. 22, no. 5, pp. 239–241, May 2012.
[18] J. Detaint and R. Lancon, "Temperature characteristics of high frequency lithium tantalate plate," in *Proc. 30th Annu. Freq. Control Symp.*, Atlantic City, NJ, USA, 1976, pp. 132–140.
[19] B. Ivira, P. Benech, R. Fillit, F. Ndagijimana, P. Ancey, and G. Parat "Modeling for temperature compensation and temperature characterizations of BAW resonators at GHz frequencies," *IEEE Trans. Ultrason., Ferroelect., Freq. Control*, vol. 55, no. 2, pp. 421–430, Feb. 2008.